



Atomic-level flat polishing of polycrystalline diamond by combining plasma modification and chemical mechanical polishing

Song Yuan^a, Chi Fai Cheung (1)^{a,*}, Alborz Shokrani (2)^c, Zejin Zhan^{a,b}, Chunjin Wang^a

^a State Key Laboratory of Ultra-precision Machining Technology, Department of Industrial and Systems Engineering, The Hong Kong Polytechnic University, Hong Kong, China

^b Department of Mechanical and Energy Engineering, Southern University of Science and Technology, Guangdong, China

^c Department of Mechanical Engineering, University of Bath, United Kingdom

ARTICLE INFO

Article history:

Available online 21 April 2025

Keywords:

Diamond

Plasma

Polishing

ABSTRACT

This paper presents an atomic-level flat polishing method based on hydroxyl ($\bullet\text{OH}$) oxidation combining plasma modification and chemical mechanical polishing (CMP) of polycrystalline diamond (PCD). The PCD surface was firstly modified using $\bullet\text{OH}$ generated by He-based H_2O_2 plasma leading to the formation of an approximately 30 nm thick uniform oxidation layer on the PCD surface composed of carbon-oxygen mixed layer and oxygen-rich layer. Reactive force field molecular dynamics (ReaxFF MD) simulations explained the plasma modification mechanism. The modified layer was then removed using CMP resulting in an atomic-level flat surface with arithmetical mean height (S_a) of 0.366 nm.

© 2025 The Authors. Published by Elsevier Ltd on behalf of CIRP. This is an open access article under the CC BY license (<http://creativecommons.org/licenses/by/4.0/>)

1. Introduction

Diamond possesses numerous engineering properties, such as high thermal conductivity and high temperature resistance. The limitations in producing synthetic single crystal diamond (SCD) have made polycrystalline diamond (PCD) a prominent candidate for optical windows materials and heat sink bonded with silicon and GaN wafers. However, processing PCD is difficult using conventional methods due to its anisotropy and inherent defects besides extremely high hardness and wear resistance.

The initial surface of PCD with a rough pyramid shape makes it difficult to be used directly after production. As a result, surface polishing is necessary for obtaining high precision and damage free surfaces. Chemical mechanical polishing (CMP) stands as the principal approach for achieving a high-precision and damage-free surface. However, the high hardness and chemical stability of PCD imposes significant challenges in oxidizing and mechanical removal during CMP. Fenton reaction based on hydroxyl ($\bullet\text{OH}$) oxidation has attracted lots of attention in processing SCD. In this process, a mixed solution of H_2O_2 and Fe^{2+} undergoes a Fenton reaction to generate $\bullet\text{OH}$ with strong oxidation properties which is used as a polishing slurry for SCD. Yuan et al. [1] developed a homogeneous Fenton-like polishing slurry. Using this method, they reported that an arithmetic roughness (R_a) of 0.076 nm and a material removal rate (MRR) of 881 nm/h can be achieved in processing SCD. Irradiating the polishing slurry with UV light can further promote the generation of $\bullet\text{OH}$ and oxidizing SCD. UV-assisted Fenton reaction can increase material removal rate and enhance surface roughness (R_a

0.071 nm) [2]. Plasma assisted polishing was proposed by Yamamura et al. [3] where water vapor or O_2 was used as the reaction gas to produce $\bullet\text{OH}$ in vacuum. Using this approach, an R_a of 0.46 nm was produced in polishing SCD. Deng et al. [4] proposed atmospheric pressure inductively coupled plasma using Argon (Ar) and H_2O_2 as reaction gases for processing SCD. They reported arithmetical mean height (S_a) of 0.86 nm. Whilst there have been many reports on processing SCD surfaces to an atomic-scale roughness, it remains a huge challenge for PCD. Qiang et al. [5] utilized thermal-assisted dynamic friction polishing for the roughing process, successfully reducing the root mean square value (R_q) from 101 nm to 10 nm. This was followed by CMP using a polishing slurry made up of aqueous K_2FeO_4 and diamond abrasive which resulted in a final roughness of R_q 3.9 nm. Mallik et al. [6] discovered the issues of uneven and irregular polishing area caused by anisotropy when polishing PCD. Considering the anisotropy, the stress distribution in crystals is not uniform, and morphological differences between neighbouring grains make it more difficult to control surface morphology.

As a result, this paper presents a polishing method combining plasma modification and CMP to achieve atomic-scale flat surface for PCD. Inspired by previous literatures [1,2], $\bullet\text{OH}$ exhibits a positive effect on the surface roughness of SCD and plasma efficiently generates abundant $\bullet\text{OH}$, which provides new opportunities in achieving atomic-scale surface roughness for PCD. This paper makes use of a plasma-assisted method to generate $\bullet\text{OH}$ for uniformly oxidizing and modifying the PCD surfaces. CMP method is employed to remove the oxidized layer leading to atomic-scale surfaces. Moreover, reactive force field molecular dynamics (ReaxFF MD) simulations have been used to elucidate the plasma modification mechanism of PCD at the atomic level.

* Corresponding author.

E-mail address: Benny.Cheung@polyu.edu.hk (C.F. Cheung).

2. Methodology

2.1. Atomic-level flat polishing method

An in-house developed, atmospheric pressure plasma jet was used for surface modification. The plasma is powered by a radio frequency power supply (13.56 MHz) and is generated through a capacitively coupled design. Two wedge-shaped electrodes in parallel generate an intensive electric field in an alumina tube, where Helium (He) and H_2O_2 flow through, leading to $\bullet\text{OH}$ plasma ignition and reactive radical generation. Modifying the PCD surface using $\bullet\text{OH}$ generated through plasma excitation of H_2O_2 reduces the material hardness and disrupts the stable chemical structure of diamond. Additionally, it oxidizes the surface resulting in a uniform oxide layer, which provides an excellent processing environment for subsequent CMP. The configuration of plasma and CMP equipment for PCD are shown in Fig. 1. Fig. 1(a) shows the plasma equipment used in this investigation as well as its principle. A PCD sample with a dimension of $10\text{ mm} \times 10\text{ mm} \times 0.5\text{ mm}$ was placed 3 mm below the plasma nozzle. The flow rate of 2 slm (standard liter per minute) was controlled using a mass flow controller. PCD was processed by plasma for 1 hour at the condition of H_2O_2 0.6 slm, He 1.4 slm, 110 W, the plasma parameters are optimized by plasma experiments to achieve efficient modification rate and high stability. As shown in Fig. 1(b), this was followed by CMP processing using a CMP-TriboLab machine (Bruker Nano, Inc). During the CMP process, the PCD sample is placed on the polyurethane polishing pad under the load of 10 N, the polishing slurry, consisting of cerium oxide (CeO_2) abrasive and aqueous H_2O_2 , drops into polyurethane polishing pad with a flow of 10 ml/min, the polishing disc rotates with a speed of 50 r/min for 1 h.

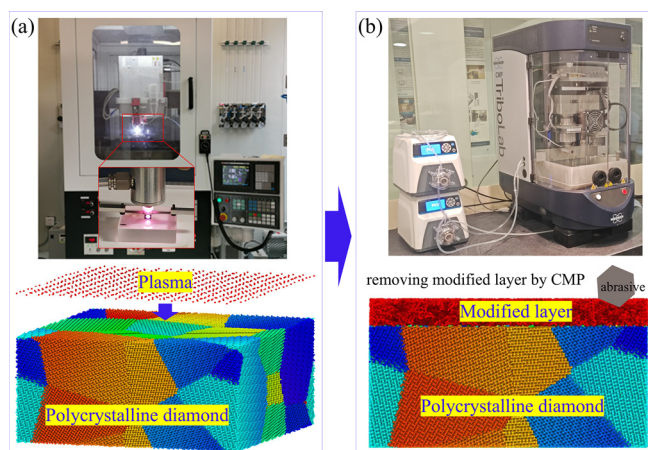


Fig. 1. The configuration of plasma (a) and CMP (b) equipment for PCD.

2.2. ReaxFF MD simulations

ReaxFF MD is a powerful computational approach for studying complex chemical reactions at the atomic scale, which bridges the gap between classical molecular dynamics (MD) and quantum mechanics. It enables performing accurate and efficient simulations of diverse chemical systems [7]. In this study, ReaxFF MD was configured to investigate plasma process of PCD. The PCD model consisting of different crystallography planes with a size of $8\text{ nm} \times 8\text{ nm} \times 4\text{ nm}$ was built using Atomsk software. During the plasma process, He-based H_2O_2 plasma was represented through $\bullet\text{OH}$ as its ultimate product. The $\bullet\text{OH}$ was given different incident energies to describe the real plasma process. In this simulation, the oncoming $\bullet\text{OH}$ atoms appeared randomly 10 Å above the surface, and the vaporization region where the atoms are dismissed is set to avoid hindering subsequent sputtering atoms. The simulation is given as follows: the PCD model was equilibrated for 20 ps until the potential energy of the system came to stability. Irradiate $\bullet\text{OH}$ from 1 nm above the PCD substrate randomly for 100 ps with an interval of 0.5 ps, that is enough to modify the whole surface region of PCD. The equilibrium phase commences within the canonical (NVT)

ensemble at 300 K using a time step of 0.25 ps. The system's temperature was maintained at 300 K with a coefficient of 25 fs. The C/H/O potential function was utilized to acquire a detailed atomic-level comprehension of the etching process of diamond subjected to energetic atomic oxygen collisions [8]. The ReaxFF MD computations were executed using LAMMPS software, while the Open Visualization Tool was employed for visualization and subsequent analysis.

3. Results and discussion

3.1. Analysis of surface morphology after plasma modification

First, the PCD surfaces were irradiated with H_2O_2 plasma to modify their surface morphology. To better understand the impact of plasma modification on PCD surface morphology, XPS, HRTEM and STEM are analysed for PCD surface after plasma modification from different perspectives. Scanning Electron Microscopy (SEM) was employed. The low magnification SEM image of the initial surface in comparison with the plasma modified sample in Fig. 2(a) clearly shows that there are numerous oxidation layers after plasma modification. The distribution of carbon (C) and oxygen (O) was investigated using energy dispersive spectrometer (EDS) demonstrating a clear distinction between the untreated area with high carbon concentration and the area rich in oxygen associated with plasma modification in Fig. 2(b) and Fig. 2(c), respectively.

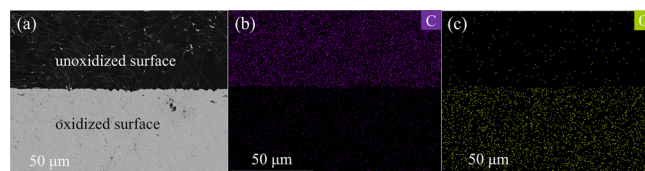


Fig. 2. Surface morphology of PCD after plasma modification. (a) contrast between the modified and untreated area, (b) distribution of C element, (c) distribution of O element.

X-ray Photoelectron Spectroscopy (XPS) was used to investigate the chemical structure and composition on the PCD surface before and after plasma treatment as shown in Fig. 3. Fig. 3(a) shows one main peak at 284.8 eV, corresponding to $\text{sp}^3\text{ C-C}$ chemical bonds. Fig. 3(b) highlights four main peaks at 288.72 eV, 286.34 eV, 284.8 eV, and 284.09 eV, corresponding to C=O , $\text{sp}^3\text{ C-C}$, and $\text{sp}^2\text{ C-C}$ chemical bonds, respectively. The XPS results of C_{1s} show that C-O , C=O , and $\text{sp}^2\text{ C-C}$ are the main chemical structure of oxidation layer, proving that the plasma treatment has oxidized the PCD surface. In comparison to the initial surface, the content of $\text{sp}^3\text{ C-C}$ chemical structure has a slight decrement. A new chemical structure, disorder C-C , occurs in PCD substrate. The presence of disordered C-C bonds signifies the disruption of the stable diamond structure, which is removed in subsequent polishing.

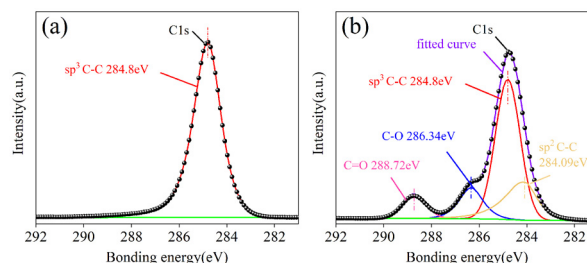


Fig. 3. The XPS spectrum of C_{1s} of PCD surface before and after plasma modification. (a) XPS spectrum of C_{1s} before, (b) XPS spectrum of C_{1s} after.

3.2. Identification of the modification mechanism after plasma

High-Resolution Transmission Electron Microscopy (HRTEM) was used to identify the modification mechanism induced by $\bullet\text{OH}$. The plasma modified PCD surface was coated with platinum and a cross section was produced using focused ion beam (FIB) milling. As shown

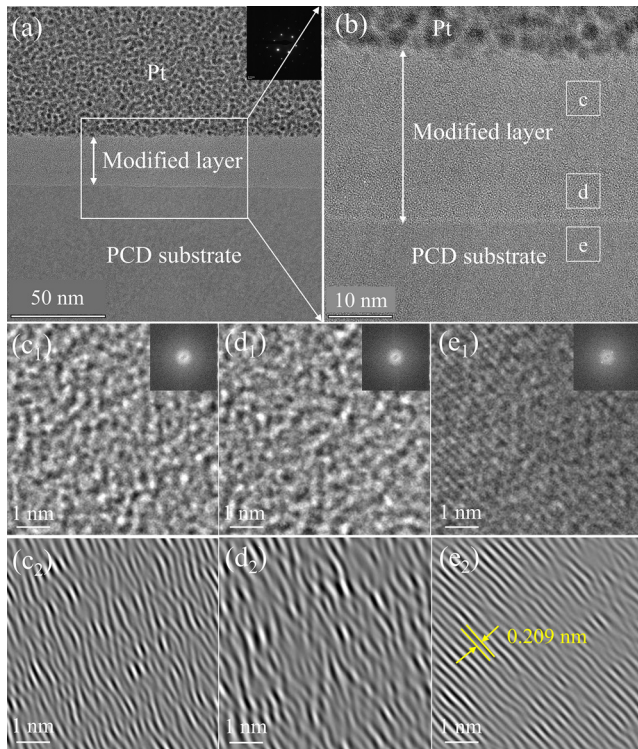


Fig. 4. HRTEM image of PCD surface after plasma modification. (a) the cross-section view of PCD substrate, (b) the high magnification image of modified layer, (c₁)–(e₁) the corresponding FFT images marked c, d, and e region in (b) respectively, (c₂)–(e₂) the corresponding IFFT images of (c₁)–(e₁).

in Fig. 4(a), there is a uniform modified layer between Pt layer and PCD substrate in broad field of vision. This demonstrates the modified layer exists across the entirety of the sample surface. The high magnification image shown in Fig. 4(b), indicates a uniform modified layer near the PCD substrate that is atomically flat at the modified layer-PCD interface. Three regions labelled c, d, and e in Fig. 4(b) are contrasted. Figs. 4(c₁–e₁) show the fast Fourier transform (FFT) of these regions followed by Figs. 4(c₂–e₂) demonstrating the inverse FFT (IFFT) images of the regions. The FFT and IFFT images of the HRTEM in Fig. 4(c₁) and Fig. 4(c₂), in which the primary structures are amorphous and a fraction of oriented lattice fringes, and the corresponding FFT pattern proves the amorphous feature exhibited as the wide diffraction ring in the upper right corner. In Fig. 4(d₁) and Fig. 4(d₂), the absence of noticeable lattice streaks signifies the disruption and amorphization of the PCD lattice. In contrast, the FFT image in Fig. 4(e₁) and the IFFT image in Fig. 4(e₂) distinctly reveal the diamond lattice with a crystallographic spacing of 0.209 nm. The corresponding FFT pattern displays sharp diffraction spots without any amorphous rings, indicating the pristine diamond lattice structure of the PCD substrate.

Scanning Transmission Electron Microscopy (STEM) was used to explore the composite and structure of the modified layer. A bright field (BF) STEM image in Fig. 5(a) shows that an even mixed layer is formed in the modified layer. The brightest area corresponds to the modified layer located at the middle of the image. There exists an obvious distinction between the modified layer and PCD substrate. The elemental distribution on the measured surface is detected by EDS proving the presence of oxygen atoms in the modified layer. The modified layer consists of two distinct sides: (i) near the top surface and (ii) near the substrate. As shown in Fig. 5(b), the top surface is rich in carbon with oxygen atoms dispersed throughout. The area closer to the substrate has significantly higher concentration of oxygen with lower carbon content. Fig. 5(c) shows the elemental distribution intensity profile of the modified layer, while the white dash-dotted line in Fig. 5(b) indicates the direction and extent of the electron energy loss spectroscopy (EELS) spectrum. The C and O elemental signal profile shows strong distribution in the range of 9 nm to 28 nm. This region corresponds to the region II in Fig. 5(a). The O elemental signal profile shows strong distribution in the range of 28 nm to

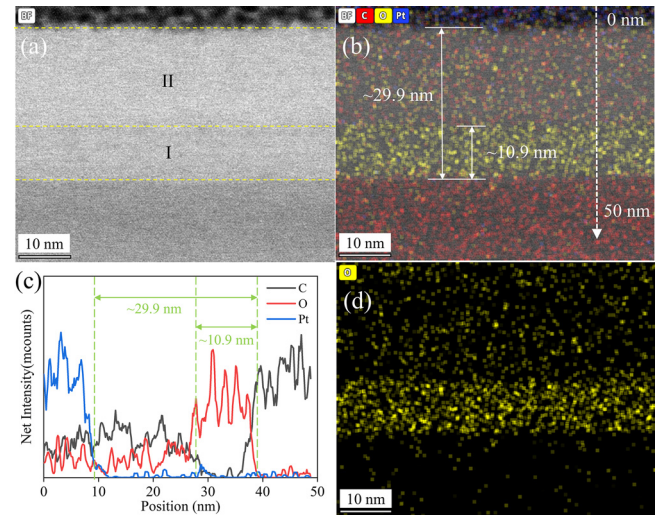


Fig. 5. STEM analysis of PCD after plasma modification. (a) the cross-sectional image of BF-STEM, (b) the BF-EDS mapping of (a), (c) the intensity profiles of C, O, and Pt in the modified layer delineated by white dotted arrow in (b), (d) the EDS mapping of O element of (a).

39 nm. This O region corresponds to the region I in Fig. 5(a). The distribution of O element is seen intuitively from Fig. 5(d). After plasma modification, the modified layer is removed by the CMP technology.

3.3. MD simulation of modification mechanism of PCD plasma treatment

At present, it is still not clear why the modified layer was generated after plasma treatment. A better understanding of the mechanism of plasma modification is deemed crucial for producing atomically flat surfaces. In the present study, ReaxFF MD simulations were developed to further explain the mechanism of plasma modification of PCD surface.

The bonding energy of C—C is 3.6 eV which is the theoretical minimum energy required for breaking a single C—C bond. As such, three incident energies of 10 eV, 20 eV, and 30 eV were chosen for the simulations, which can be regarded as low, medium, and high energies, respectively. Fig. 6(a) shows the ReaxFF MD model of plasma with •OH of varying incident energies moving towards the PCD substrate. The ReaxFF MD results of the PCD modified by •OH after 100 ps with different incident energies are shown in Fig. 6(b–d). When a low incident energy of 10 eV is used, a portion of the •OH is absorbed by the topmost surface of the PCD sample upon impact as shown in Fig. 6(b). The energy is not enough to offset the C—C bonding energy, let alone breaking the C—C bonds. This may be due to the loss of energy during plasma process. As shown in Fig. 6(c), increasing the incident energy from 10 eV to 20 eV in medium energy scenario results in the penetration of •OH into the subsurface of PCD whilst still a noticeable portion is absorbed by the top surface forming chemical structures such as C—O and C = O bonds. The presence of these structures was

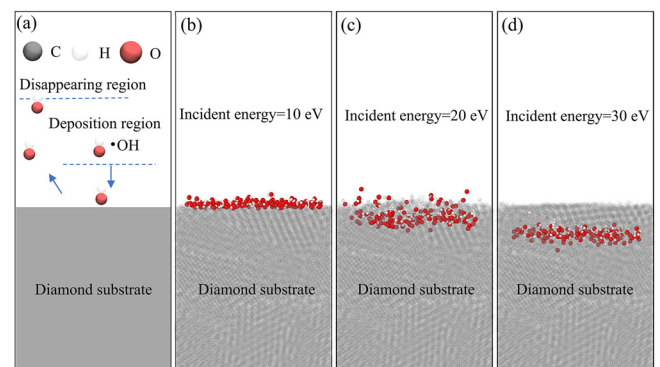


Fig. 6. Snapshots of plasma with •OH of varying incident energies moving towards the PCD substrate. (a) ReaxFF MD model of plasma, (b) plasma results at 10 eV, (c) plasma results at 20 eV, (d) plasma results at 30 eV.

also confirmed in the experimental XPS results in Fig. 3(a). When the incident energy rises to 30 eV, the sp^3 C—C bonds are dissociated and some distorted C_xO_y structures are formed in the PCD subsurface, as demonstrated in Fig. 6(d). The model clearly shows that when a high level of incident energy is used, the $\bullet OH$ can penetrate the PCD surface forming a thick oxidation layer after exposure to H_2O_2 plasma for 100 ps. This thick oxide layer below the PCD surface was confirmed by STEM as shown in Fig. 5(b).

The ReaxFF MD simulations show that when the incident energy of $\bullet OH$ is low, they are absorbed by the PCD surface and fail to overcome the bonds between the carbon atoms. At a critical point, 20 eV in this case, they can break the C—C bonds and form oxides on the surface of the sample. Further increasing the incident energy, $\bullet OH$ can penetrate the surface and form oxides below the surface by dissociating the sp^3 C—C and forming C_xO_y structures. Besides, an obvious boundary that can be observed between the oxidation layer and the intact diamond substrate, numerous $\bullet OH$ are deposited on the boundary near the oxidation layer. As a result, some C_xO_y structures occur above the $\bullet OH$ deposition region, which is also consistent with the TEM results. The effects of H_2O_2 plasma treatment of PCD are divided into three types namely, (i) adsorption of $\bullet OH$ on the topmost surface, (ii) adsorption of $\bullet OH$ and dissociation of C—C bonds on the topmost surface, and (iii) penetration of $\bullet OH$ and dissociation of C—C bonds. These stages appear to be governed by the incident energy of $\bullet OH$ and the simulation results explain why the modified layer occurs.

Whilst the simulation results show clear distinction between the PCD subject to different incident energies, the experimental observation shows a mixture of the three plasma treatment types. During the PCD plasma modification, abundant $\bullet OH$ are produced by H_2O_2 plasma. Unlike in the simulation, where an exact value for the incident energy is defined, not all $\bullet OH$ have identical incident energies. Instead, their energies vary within a range with a mean value. As such, a mix of different plasma treatment types can be observed in the experimental sample as shown in Fig. 5. At atomic scale, the effect of each $\bullet OH$ is different to another upon impacting the PCD surface depending on their energy.

Due to the chemical stability of diamond, it is difficult to form a thick oxide layer. Even if the diamond is immersed in an oxidizing agent for an extended period, the oxidized layer only forms on the topmost layer [1]. In contrast, plasma modification presents an opportunity to modify the subsurface of the PCD by generating an oxidized layer below the surface. After plasma modification, the crystal grains translate into amorphous C_xO_y structures and can be oxidized. The whole surface adsorbs more $\bullet OH$ layer by layer and a thick oxidation layer is formed finally.

3.4. Surface morphology after plasma assisted CMP

The H_2O_2 plasma treated PCD surface was polished by CMP to obtain an atomic scale surface. To demonstrate the polishing results, the optical morphology and Atomic Force Microscope (AFM) morphology are compared between the initial surface before in Fig. 7(a–b) and the final surface after in Fig. 7(c–d), the Sa 0.643 nm of PCD with the measurement area of $841.5 \mu m \times 841.5 \mu m$ is achieved after plasma assisted CMP. The AFM results demonstrate that a smoother surface roughness Sa of 0.366 nm is obtained by plasma assisted CMP compared with the initial Sa 4.190 nm, even though there exist clear grain boundaries between crystal grains in Fig. 7(d). The AFM results revealed that the grain boundaries are the main hinderance in effective polishing of PCD.

4. Conclusions

Conventional polishing of PCD for achieving atomic-scale surfaces is challenging due to the presence of grain boundaries inhibiting effective mechanical removal. In this paper, a flat polishing method for producing PCD with atomic-level surface finish is presented. It is based on $\bullet OH$ oxidation combining H_2O_2 plasma modification of PCD surface and subsurface followed by CMP. The AFM results demonstrated that the arithmetical mean height Sa 0.366 nm can be achieved using the proposed method despite the presence of clear

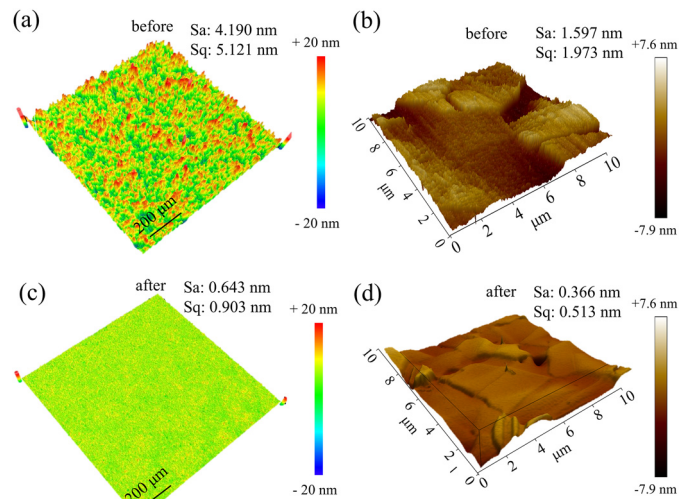


Fig. 7. Surface morphology before and after plasma assisted CMP. (a) optical morphology before: Sa : 4.190 nm, Sq : 5.121 nm, (b) AFM morphology before: Sa : 1.597 nm, Sq : 1.973 nm, (c) optical morphology after: Sa : 0.643 nm, Sq : 0.903 nm, (d) AFM morphology after: Sa : 0.366 nm, Sq : 0.513 nm.

grain boundaries between crystal grains. According to the experimental and simulation results, the plasma modification can be summarized as follows: by exciting aqueous H_2O_2 to generate numerous $\bullet OH$ with different incident energies, the oxidation layer including extensive oxygen can be observed on the PCD surface after plasma modification. C—O, C = O, and sp^2 C—C are the main chemical structure of oxidation layer. STEM and HRTEM results revealed the presence of a uniform modified layer on the PCD surface, with a thickness of approximately 30 nm, the modified layer consists of carbon-oxygen mixed layer and oxygen-rich layer. The modified layer can be easily removed using chemical-mechanical polishing leading to an atomic-level flat surface with sub-nanometric surface finish.

Declaration of competing interest

The authors declare that they have no known competing financial interests or personal relationships that could have appeared to influence the work reported in this paper.

CRediT authorship contribution statement

Song Yuan: Writing – review & editing, Writing – original draft, Visualization, Validation, Methodology, Investigation, Formal analysis, Data curation, Conceptualization. **Chi Fai Cheung:** Writing – review & editing, Writing – original draft, Visualization, Validation, Supervision, Resources, Project administration, Methodology, Investigation, Funding acquisition, Formal analysis, Conceptualization. **Alborz Shokrani:** Writing – review & editing, Writing – original draft, Validation, Methodology, Investigation, Formal analysis, Data curation, Conceptualization. **Zejin Zhan:** Writing – review & editing, Visualization, Validation, Methodology, Investigation, Formal analysis, Conceptualization. **Chunjin Wang:** Writing – review & editing, Writing – original draft, Validation, Supervision, Methodology, Investigation, Formal analysis, Conceptualization.

Acknowledgments

The authors would like to express thanks to the National Key R&D Program of China (No. 2023YFE0203800), Innovation and Technology Commission (ITC) of the Government of the HKSAR, China (MHP/151/22), Guangdong Basic and Applied Basic Research Foundation (2025A1515011366), and Postdoc Matching Fund Scheme of The Hong Kong Polytechnic University (1-W29X). The authors acknowledge the Beijing Super Cloud Computing Center (BSCC) for providing HPC resources that have contributed to the research results reported within this paper. The authors also thank Prof. Hui Deng from Southern University of Science and Technology for his strong support to this paper.

References

- [1] Yuan S, Guo X, Li M, Jin Z, Guo D (2022) An insight into polishing slurry for high quality and efficiency polishing of diamond. *Tribol Int* 174:107789.
- [2] Yuan S, Guo X, Wang H, Gao S (2023) A theoretical and experimental study on high-efficiency and ultra-low damage machining of diamond. *Journal of Manufacturing Science and Engineering-ASME* 145:071006.
- [3] Yamamura K, Emori K, Sun R, Ohkubo Y, Endo K, Yamada H, Chayahara A, Mokuno Y (2018) Damage-free highly efficient polishing of single-crystal diamond wafer by plasma-assisted polishing. *CIRP Annals* 67:353–356.
- [4] Luo H, Ajmal KM, Liu W, Yamamura K, Deng H (2021) Atomic-scale and damage-free polishing of single crystal diamond enhanced by atmospheric pressure inductively coupled plasma. *Carbon N Y* 182:175–184.
- [5] Qiang, M., Chen, S., YIN, X., Wu, L., Fan, Y., Xu, X., Wang, Z., Dun, A. (2024), Two-step polishing progress and mechanism for polycrystalline diamond, preprints.opticaopen.org.
- [6] Mallik AK, Bhar R, Bysakh S (2016) An effort in planarising microwave plasma CVD grown polycrystalline diamond (PCD) coated 4 in. Si wafers. *Mater Sci Semicond Process* 43:1–7.
- [7] Van Duin AC, Dasgupta S, Lorant F, Goddard WA (2001) ReaxFF: a reactive force field for hydrocarbons. *The Journal of Physical Chemistry A* 105:9396–9409.
- [8] Chenoweth K, Van Duin AC, Goddard WA (2008) ReaxFF reactive force field for molecular dynamics simulations of hydrocarbon oxidation. *The Journal of Physical Chemistry A* 112:1040–1053.